HHS Public Access

Author manuscript

Cell Metab. Author manuscript; available in PMC 2018 February 07.

Published in final edited form as:

Cell Metab. 2017 February 07; 25(2): 358–373. doi:10.1016/j.cmet.2016.12.010.

Prevention of dietary fat-fueled ketogenesis attenuates BRAF V600E tumor growth

Siyuan Xia[1], **Ruiting Lin**[1], **Lingtao Jin**[1], **Liang Zhao**[1], **Hee-Bum Kang**[1], **Yaozhu Pan**[1], **Shuangping Liu**[1], **Guoqing Qian**[1], **Zhiyu Qian**[1], **Evmorfia Konstantakou**[1], **Baotong Zhang**[1], **Jin-Tang Dong**[1], **Young Rock Chung**[3], **Omar Abdel-Wahab**[3], **Taha Merghoub**[3], **Lu Zhou**[4], **Ragini R. Kudchadkar**[1], **David H. Lawson**[1], **Hanna J. Khoury**[1], **Fadlo R. Khuri**[1], **Lawrence H. Boise**[1], **Sagar Lonial**[1], **Benjamin H. Lee**[5], **Brian P. Pollack**[6,7], **Jack L. Arbiser**[6,7], **Jun Fan**[2,8], **Qun-Ying Lei**[4,8], and **Jing Chen**[1,8,9]

[1]Department of Hematology and Medical Oncology, Winship Cancer Institute of Emory, Emory University School of Medicine, Atlanta, Georgia, 30322, USA. Emory University, Atlanta, Georgia 30322, USA.

[2]Department of Radiation Oncology, Winship Cancer Institute of Emory, Emory University School of Medicine, Atlanta, Georgia, 30322, USA. Emory University, Atlanta, Georgia 30322, USA.

[3]Memorial Sloan-Kettering Cancer Center, New York, NY 10065, USA.

[4]Fudan University, Shanghai 201203, China.

[5]Novartis Institutes for BioMedical Research, Cambridge, Massachusetts 02139, USA.

[6]Department of Dermatology, Emory University, Atlanta, Georgia 30322, USA.

[7]Atlanta Veterans Administration Medical Center, Atlanta, Georgia 30322, USA.

SUMMARY

Lifestyle factors including diet play an important role in the survival of cancer patients. However, the molecular mechanisms underlying pathogenic links between diet and particular oncogenic mutations in human cancers remain unclear. We recently reported that the ketone body acetoacetate selectively enhances BRAF V600E mutant-dependent MEK1 activation in human cancers. Here we show that a high-fat ketogenic diet increased serum levels of acetoacetate, leading to enhanced tumor growth potential of BRAF V600E-expressing human melanoma cells in

[8]Correspondence to: jfan3@emory.edu (J.F.), qlei@fudan.edu.cn (Q.-Y.L.) or jchen@emory.edu, (J.C.).
[9]Lead Contact

SUPPLEMENTAL INFORMATION

Supplemental Information includes Extended Experimental Procedures, 7 figures and 1 table.

Author Contributions

S.X., R.L., J.F. designed and performed the majority of experiments. Y.R.C., O.A.-W., T.M., R.R.K., D.H.L., S. Lonial, H.J.K., F.R.K., L.H.B., B.P.P., and J.L.A. provided critical reagents. L.Z. and Q.L. performed structural analysis. B.H.L. performed the histopathological analyses. B.Z. and J.-T.D. assisted with IHC studies. L.J., L.Z., H.-B.K., Y.P., S. Liu, G.Q., Z.Q., and E.K. performed all of the other experiments. S.X., F.J., B.P.P, J.L.A. and J.C. designed the study. S.X., J.F., Q.-Y. L. and J.C. managed the project and wrote the paper.

xenograft mice. Treatment with hypolipidemic agents to lower circulating acetoacetate levels or an inhibitory homologue of acetoacetate, dehydroacetic acid, to antagonize acetoacetate-BRAF V600E binding attenuated BRAF V600E tumor growth. These findings reveal a signaling basis underlying a pathogenic role of dietary fat in BRAF V600E-expressing melanoma, providing insights into the design of conceptualized “precision diets” that may prevent or delay tumor progression based on an individual’s specific oncogenic mutation profile.

Graphical Abstract

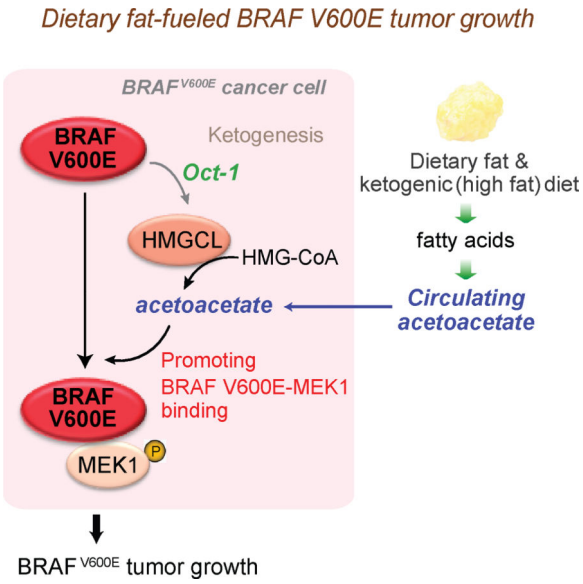

INTRODUCTION

The link between diet and cancer prevention is well supported by a large amount of data derived from diverse epidemiological studies as well as preclinical studies using experimental animals. Overall, despite a poor understanding of the complex interactions of diverse dietary components, these epidemiological studies consistently support inverse relationships between cancer risk and intake of “healthy food” such as vegetables, fruits, whole grains and dietary fiber, and direct relationships between cancer risk and dietary fat as well as other “calorie-dense food” such as deep fried food and processed meat [reviewed in (Greenwald et al., 2001; Miller, 1990)]. However, these epidemiological studies are more descriptive than mechanistic in nature, and many questions remain to be resolved. It is unclear, for example, which specific dietary factors are predominantly important in providing a cancer prevention effect and how they may function alone and/or interact with other dietary factors to control cancer risk in all or specific cancer types. Most importantly, although epidemiological data suggest a general connection between diet and cancer risk, pathogenic links between diet and particular oncogenic mutations in certain cancer types remain unknown.

Understanding the molecular details of metabolic alterations in cancer may suggest connections between cancer risk and certain diets that fuel cancer-related metabolic changes,

which are informative to the development and design of diets that can lower cancer risk and improve treatment. For example, increasing evidence suggests that different human cancers may share common metabolic properties such as the Warburg effect, in which cancer cells avidly consume glucose (Kim and Dang, 2006; Kroemer and Pouyssegur, 2008), suggesting that cancer may thrive on sugar and thus a sugar-depleted “diet therapy” may lower cancer risk. In fact, a ketogenic diet (high-fat, adequate-protein and low-carbohydrate) has been evaluated for cancer prevention and treatment purposes to attenuate tumor development by limiting carbohydrate supply (Tennant et al., 2010). However, the clinical efficacy of such diet therapies may vary due to the fact that distinct oncogenic backgrounds in different cancer types require different metabolic properties for tumor development.

We recently performed a systematic RNAi-based screen and identified metabolic vulnerabilities specifically required by oncogenic BRAF V600E mutant, but not other oncogenes such as NRAS Q61R/K, in human melanoma (Kang et al., 2015). More than 50% of melanomas express BRAF V600E mutant, which represents a therapeutic target due to its pathogenic role (Bollag et al., 2012; Gibney et al., 2013; Johnson and Sosman, 2013). Moreover, BRAF V600E mutation is also found in 10% of colorectal cancer (Benlloch et al., 2006; Sebolt-Leopold and Herrera, 2004), 100% of hairy cell leukemia (HCL) (Arcaini et al., 2012) and 5% of multiple myeloma (Chapman et al., 2011) cases. We found that HMG-CoA lyase (HMGCL), a key enzyme in ketogenesis producing ketone bodies, is selectively essential in melanoma cells expressing BRAF V600E (Kang et al., 2015). Ketogenesis mainly occurs in the mitochondria of liver cells, which normally produce ketone bodies as a result of fatty acid breakdown to generate energy when glucose levels in the blood are low (Balasse and Fery, 1989; McPherson and McEneny, 2012). HMGCL converts HMG-CoA to acetyl-coA and a ketone body, acetoacetate, which can be further converted to two other ketone bodies, including D-β-hydroxybutyrate (3HB) and acetone (Cotter et al., 2013; Morris, 2005). We found that oncogenic BRAF V600E upregulates HMGCL gene expression in cancer cells. HMGCL in turn selectively promotes BRAF V600E-dependent phosphorylation and activation of MEK1 by controlling intracellular levels of its product acetoacetate, which specifically promotes BRAF V600E (but not BRAF WT) binding to MEK1 (Kang et al., 2015). These results support an emerging “metabolic rewiring” concept in which distinct oncogenes may require different metabolic alterations for tumor growth.

Moreover, our findings suggest that a ketogenic diet would likely worsen the disease burden in BRAF V600E-positive cancer patients. Since acetoacetate is cell permeable (Kang et al., 2015), herein we tested a hypothesis that, in addition to the increased intracellular acetoacetate levels induced by BRAF V600E, dietary fat-fueled ketogenesis may promote BRAF V600E melanoma growth *in vivo* through increased circulating and consequently intracellular levels of acetoacetate.

RESULTS

High dietary fat elevates serum acetoacetate to promote BRAF V600E tumor growth

We found that high-fat diets in either solid or paste forms resulted in increased growth rates, masses and sizes of tumors without affecting body weight in nude mice with BRAF V600E-expressing human melanoma A375 cell xenografts (Figures 1A and S1A; *upper* panels). In

contrast, a high-fat diet did not affect tumor growth rates, masses or sizes or body weight in mice with control SK-MEL-2 tumor xenografts expressing an active NRAS Q61R mutant (Figure 1A and S1A; *lower panels*). The increased tumor growth in A375 xenograft mice fed a high-fat diet was not due to differences in food intake amounts (Figure S1B). In both A375 and SK-MEL-2 models, consumption of a high-fat diet did not significantly affect serum levels of D-β-hydroxybutyrate (3HB) (Figure 1C), but significantly increased serum cholesterol levels (Figure 1D) and reduced serum glucose levels (Figure S1C), compared to control mice fed with normal food. Serum levels of acetoacetate were also increased in both A375 and SK-MEL-2 xenograft mice fed with high-fat diets (Figure 1B). The increased serum levels of acetoacetate led to enhanced phosphorylation of MEK1 and ERK1/2 without affecting HMGCL expression (Figure 1E), as well as increased binding between BRAF V600E-MEK1 (Figure 1F) in tumors derived from A375 cells but not control SK-MEL-2 cells, compared to corresponding control xenograft mice fed with normal food. Consistent with these findings, consumption of a high-fat diet resulted in increased cell proliferation rates in tumors derived from A375 cells but not control SK-MEL-2 cells, assessed by increased immunohistochemistry (IHC) staining of Ki67, compared to corresponding control xenograft mice fed with normal food (Figures 1G and S1D). Similar results were obtained in nude mice carrying BRAF V600E-expressing human melanoma A2058 xenograft tumors compared to mice with control PMWK cell xenografts expressing BRAF wild-type (WT) or HMCB cell xenografts expressing an active NRAS Q61K mutant (Figure S1E–S1J).

Intraperitoneal injection with acetoacetate but not 3HB promotes BRAF V600E tumor growth

We found that intraperitoneal injection with acetoacetate but not 3HB resulted in increased growth rates and masses of tumors derived from BRAF V600E-expressing A375 melanoma cells in xenograft nude mice (Figure 2A; *upper left* and *right*, respectively). In contrast, injection with either acetoacetate or 3HB had no effect on growth rates or masses of tumor xenografts derived from control NRAS Q61K-expressing HMCB cells (Figure 2A; *lower left* and *right*, respectively).

We chose to use the lithium salt form of acetoacetate, which provides the anion form of acetoacetate that is approximately 55 times more stable with a half-life of 130 hours than the acid form (acetoacetic acid) with a half-life of 140 minutes at 37°C in water (Hay, 1967). To exclude potential effects of the lithium ion, we performed a series of experiments using a control salt lithium chloride. We found that lithium chloride did not bind to purified BRAF V600E in a thermal shift assay (Figure S2A) or promote the association between purified BRAF V600E and MEK1 (Figure S2B) as acetoacetate does. Consistently, treatment with lithium chloride did not affect phosphorylation levels of MEK1 or ERK1/2, BRAF V600E-MEK1 binding, or cell proliferation rates in diverse BRAF V600E positive or negative human melanoma cells (Figure S2C–S2E, respectively). Moreover, lithium chloride treatment did not affect tumor growth potential of BRAF V600E-expressing A375 cells in xenograft mice *in vivo* (Figure S2F), nor did it affect serum levels of acetoacetate, 3HB, cholesterol or glucose (Figure S2G), phosphorylation levels of MEK1 or ERK1/2, BRAF V600E-MEK1 binding, or cell proliferation potential in tumors derived from A375 cells in xenograft mice (Figure S2H–S2J, respectively). In addition, similar studies were performed

to exclude possible effects from the potential degradation product of acetoacetate, acetone. We found that acetone did not bind to purified BRAF V600E in both thermal shift assay and a binding assay using ^{14}C-labeled acetone (Figure S3A, *left* and *right*, respectively) or affect the association between purified BRAF V600E and MEK1 (Figure S3B). Acetone also did not affect phosphorylation levels of MEK1 or ERK1/2, BRAF V600E-MEK1 binding, or cell proliferation rates in diverse BRAF V600E positive or negative human melanoma cells (Figure S3C–S3E, respectively). These results, together with our previous finding that ^{14}C-labeled acetoacetate binds to purified BRAF V600E (Kang et al., 2015), suggest that the anion form of acetoacetate is the functional compound that binds to and regulates BRAF V600E.

Consistently, intraperitoneal injection with acetoacetate led to increased serum levels of acetoacetate (Figure 2B) but did not affect serum levels of 3HB (Figure 2C), whereas 3HB injection increased serum levels of β-hydroxybutyrate (Figure 2C) but not acetoacetate (Figure 2B). Similarly, chronic injection of acetoacetate or 3HB to nude mice for 4 weeks resulted in increased serum acetoacetate but not 3HB levels or increased 3HB but not acetoacetate levels, respectively (Figure S3F). Such chronic treatments to mice did not alter the acetoacetate or 3HB levels in urine (Figure S3G), suggesting the dosages of acetoacetate and 3HB were insufficient to induce acidosis in mice. Moreover, injection of mice carrying A375 xenografts with acetoacetate but not 3HB resulted in enhanced phosphorylation of MEK1 and ERK1/2 (Figure 2D), enhanced BRAF V600E-MEK1 association (Figure 2E), increased tumor sizes (Figure S3H), and enhanced cell proliferation rates assessed by increased Ki67 IHC staining (Figures 2F and S3I). In contrast, in mice with HMCB xenografts, injection of either acetoacetate or β-hydroxybutyrate did not affect MEK-ERK activation (Figure 2D), BRAF–MEK1 binding (Figure 2E) or cell proliferation rates (Figures 2F and S3I) in harvested tumors. Together, these data suggest that dietary fat likely promotes tumor growth potential of BRAF V600E-expressing melanoma cells *in vivo* through elevation of serum levels of acetoacetate.

Hypolipidemic agents attenuate BRAF V600E tumor growth by reducing serum levels of acetoacetate

We next examined whether treatment with hypolipidemic agents may attenuate circulating acetoacetate levels and consequently BRAF V600E tumor growth potential in mice. We chose three drugs that are clinically used to treat hypercholesterolemia, including fluvastatin that belongs to a class of cholesterol-lowering statins as HMG-CoA reductase inhibitors (Avis et al., 2007); niacin (a.k.a. vitamin B3) that lowers triglycerides and is also clinically used to treat cardiovascular patients not taking a statin (Jacobson et al., 1994); and fenofibrate, a fibric acid derivative that also lowers triglycerides (Superko, 1989).

We found that fluvastatin and niacin treatment effectively attenuated tumor growth potential of BRAF V600E-expressing A375 cells in xenograft mice, which could be reversed by intraperitoneal injection with acetoacetate (Figure 3A, *top*; and Figure S4A, *left*). Similarly, treatment with fenofibrate attenuated tumor growth potential of BRAF V600E-expressing A2058 melanoma cells in xenograft nude mice (Figure 3A, *middle* and Figure S4A, *upper right*), but not control mice injected with NRAS Q61K-expressing HMCB cells (Figure 3A,

bottom and Figure S4A, *lower right*). Intraperitoneal acetoacetate injection effectively rescued the decreased tumor growth of A2058 cells in mice treated with fenofibrate but had no effect on tumor growth potential of HMCB cells in xenograft mice. Consistent with these findings, treatment with fluvastatin, niacin or fenofibrate resulted in reduced serum levels of acetoacetate but not β-hydroxybutyrate in mice (Figures 3B and 3C, respectively), while acetoacetate injection rescued the decreased serum acetoacetate levels but did not affect 3HB levels. Although these three drugs did not affect serum glucose levels (Figure S4B) or body weight (Figure S4C) of mice and only niacin treatment resulted in marginally decreased serum cholesterol levels that were not affected by acetoacetate injection (Figure 3D), all three hypolipidemic agents effectively reduced serum levels of triglyceride in mice despite acetoacetate injection (Figure 3E). Consistently, fluvastatin, niacin, or fenofibrate treatment resulted in decreased phosphorylation of MEK1 and ERK1/2 (Figure 3F), decreased BRAF V600E-MEK1 association (Figure 3G), and reduced cell proliferation rates as evidenced by decreased Ki67 IHC staining (Figures 3H and S4D–S4E) only in tumors derived from BRAF V600E-expressing A375 and A2058 cells but not control HMCB cells, whereas these inhibitory effects were effectively reversed by injection with acetoacetate. Similar results were obtained in fluvastatin or niacin-treated xenograft nude mice injected with A2058 cells (Figure S4F–S4H).

Discovery and characterization of dehydroacetic acid (DHAA) as an inhibitory homologue of acetoacetate

We next sought to determine whether functional inhibition of acetoacetate would attenuate BRAF V600E tumor growth. We examined a group of commercially available acetoacetate analogues and found dehydroacetic acid (DHAA) (Figure 4A) is an inhibitory homologue of acetoacetate. Similar to acetoacetate (Kang et al., 2015), DHAA also directly binds to BRAF V600E but not BRAF WT in a thermal melt shift assay using purified recombinant BRAF WT or V600E incubated with increasing concentrations of DHAA (Figure 4B). Moreover, in a cellular thermal shift assay using cell lysates from 293T cells transfected with FLAG-tagged BRAF WT or V600E, both acetoacetate (400μM) and DHAA (400μM) bound only to BRAF V600E but not WT, and DHAA bound to BRAF V600E with higher affinity than acetoacetate (Figure 4C). In addition, we performed a series of radiometric metabolite-protein interaction analyses using ^{14}C-labeled acetoacetate incubated with purified BRAF variants in the presence and absence of DHAA. As shown in Figure 4D, ^{14}C-labeled acetoacetate specifically bound to BRAF V600E and a V600E mutant of an active, truncated C-terminal domain of BRAF (tBRAF, 416–766 aa) (Brummer et al., 2006), but not to control proteins including BRAF WT, tBRAF WT or a truncated N-terminal domain of BRAF (BRAF-N, 1–415 aa), whereas treatment with DHAA resulted in a significant decrease in binding ability of BRAF V600E mutant forms to acetoacetate (Figure 4D). Additionally, DHAA competed with acetoacetate for BRAF V600E binding in a dose-dependent manner in a binding assay where purified BRAF V600E mutant pre-treated with ^{14}C-labeled acetoacetate was incubated with increasing concentrations of DHAA (Figure 4E). Furthermore, pre-treatment of purified BRAF V600E mutant with DHAA (200μM) was sufficient to block acetoacetate binding to recombinant BRAF V600E incubated with increasing concentrations of ^{14}C-labeled acetoacetate up to 400μM (Figure 4F).

These data together suggest that DHAA binds to BRAF V600E with a higher affinity that enables DHAA to compete with acetoacetate for V600E binding. Consistently, we found that ^{14}C-labeled acetoacetate bound only to BRAF proteins harboring different substitutions of V600 including clinically reported V600E, V600D and V600R with Kd values determined as approximately 92μM, 93μM and 113μM, respectively, but not to a negative control mutant V600A or to other clinically reported BRAF mutants including L597Q and K601E (Figure 4G, *left*). Moreover, DHAA effectively competed for AA binding with BRAF V600E, V600D and V600R in the presence of 300μM ^{14}C-labeled acetoacetate with Ki values determined as approximately 88μM, 88μM and 91μM, respectively (Figure 4G, *right*). These findings are also consistent with results from a binding assay using ^{14}C-labeled acetoacetate incubated with diverse BRAF mutants, where acetoacetate bound to V600E, V600D and V600R but not to control V600A mutant or other clinically reported BRAF mutants including K507E, N581S, D594N, L597Q, K601E, and S616F (Figure S5A, *upper*), and acetoacetate promoted MEK1 binding to BRAF V600E, V600D and V600R with increased MEK1 phosphorylation, but not to other BRAF mutants (Figure S5A, *lower*).

We next sought to determine whether DHAA inhibits BRAF V600E directly. Previously we demonstrated that acetoacetate binding resulted in increased Vmax and slightly decreased Km of BRAF V600E using MEK1 as a substrate (Kang et al., 2015). Interestingly, we found that treatment with increasing concentrations of DHAA alone did not affect BRAF V600E kinase activity with unaltered Vmax and Km (Figure 4H, *left*). In contrast, DHAA treatment effectively reversed the activating effect of acetoacetate on BRAF V600E in terms of increased Vmax and decreased Km of BRAF V600E in the presence of acetoacetate (300μM) when using MEK1 as a substrate (Figure 4H, *right*). Further mechanistic studies revealed that DHAA treatment effectively inhibited acetoacetate-enhanced MEK1 binding to BRAF V600E and consequent phosphorylation of V600E-bound MEK1 in a cell-free, *in vitro* coupled protein-protein binding and kinase assay using purified recombinant BRAF V600E pre-treated with acetoacetate (300μM) and incubated with recombinant purified MEK1 as a substrate (Figure 4I *right panel*). In contrast, DHAA had no effect on BRAF WT-MEK1 binding or MEK1 phosphorylation in a control experiment using purified BRAF WT incubated with MEK1 in the presence of acetoacetate (Figure 4I *left panel*). Notably, DHAA at 200μM was sufficient to compete with acetoacetate at 300μM for BRAF V600E binding (Figures 4E, 4F and 4H) and inhibit BRAF V600E-MEK1 binding and phosphorylation of MEK1 enhanced by acetoacetate at 300μM (Figure 4I). This is physiologically consistent with the acetoacetate levels determined as approximately 300μM in stable HMGCL knockdown A375 and A2058 cells (Kang et al., 2015). These results together are consistent with our hypothesis that mutation at V600 is the predominant mechanism underlying acetoacetate binding to BRAF protein, and DHAA primarily functions by competing with acetoacetate for mutant BRAF binding.

DHAA selectively inhibits cell proliferation and tumor growth potential of BRAF V600E melanoma cells

Next we found that DHAA treatment selectively inhibited cell proliferation of A375, A2058 and SK-MEL-5 cells expressing BRAF V600E and WM-266-4 cells expressing BRAF V600D (Figures 5A and S5B), but not control PMWK, CHL-1 and MeWo cells expressing

BRAF WT or HMCB and SK-MEL-2 cells expressing active NRAS mutants (Figures 5A and S5B). Consistent with these findings, DHAA treatment selectively inhibited phosphorylation of MEK1 and ERK1/2 (Figure 5B) and BRAF V600E-MEK1 association (Figure 5C) only in BRAF V600E-expressing A375 and A2058 cells but not in control PMWK or HMCB cells. The inhibitory effect of DHAA on diverse BRAF V600E-expressing cells could not be reversed by acetoacetate treatment in terms of reduced cell proliferation (Figures 5D and S5C) or decreased MEK-ERK activation (Figure 5E). Similar results were obtained using immortalized melanocyte Mel-ST cells overexpressing BRAF WT, V600E or tBRAF, where DHAA treatment selectively inhibited cell proliferation, MEK-ERK activation and BRAF V600E-MEK1 binding in BRAF V600E-expressing cells but not parental or control cells expressing BRAF WT or tBRAF (Figures 5F–5H, respectively). In addition, acetoacetate treatment did not reverse the inhibitory effect of DHAA on BRAF V600E-expressing Mel-ST cell proliferation (Figure 5I).

Consistent with these findings, DHAA treatment for ~3.5 weeks effectively inhibited tumor growth rates, sizes and masses in nude mice with BRAF V600E-expressing human melanoma A2058 and A375 cell xenografts but not in mice carrying control xenografts derived from HMCB cells expressing NRAS Q61K (Figures 6A and S6A). Notably, DHAA treatment did not affect acetoacetate or β-hydroxybutyrate levels in tumors harvested from xenograft mice (Figures 6B–6C, respectively). In contrast, DHAA treatment selectively inhibited phosphorylation of MEK1 and ERK1/2 without affecting HMGCL expression (Figure 6D), reduced binding between BRAF V600E-MEK1 (Figure 6E), and reduced cell proliferation rates as assessed by IHC staining of Ki67 (Figures 6F and S6B) in tumors derived from A2058 or A375 cells but not control HMCB cells, compared to corresponding control xenograft mice treated with water.

DHAA is a synthetic organic compound that is used mostly as a fungicide and bactericide (Stedman et al., 1954), showing little to no clinical toxicity or irritating potential and has been safely used in skin care products. Consistently, chronic injection of DHAA to nude mice for ~4 weeks revealed that 200 mg/kg/day administered intraperitoneally is a well-tolerated dose, which did not cause notable differences in histopathological analyses and weights of diverse organs (Figure S6C–S6D, respectively). Moreover, chronic treatment with DHAA had no obvious effect on the mouse gut microbiome, as evidenced by an unaltered total DNA amount extracted from bacteria in mouse feces, suggesting no change in total bacterial number in the mouse gut (Figure S6E), and by altered proportions but no loss of any components of the gut microbiota (Figure S6F). DHAA treatment did not alter complete blood counts (CBC) or hematopoietic properties in representative A375 xenograft mice compared to the water-treated group (Table S1). These results together suggest that DHAA treatment does not cause obvious toxicity *in vivo*.

Further studies revealed that the inhibitory effect of DHAA treatment on tumor growth potential of A375 cells in xenograft mice was not reversed by intraperitoneal injection with acetoacetate (Figure 6G), despite increased serum levels of acetoacetate in DHAA-treated mice receiving acetoacetate injection (Figure 6H). DHAA treatment did not affect serum levels of 3HB, cholesterol or glucose in mice in the presence or absence of acetoacetate injection (Figures 6I–6J, S6G, respectively). Consistently, acetoacetate injection did not

reverse the inhibitory effects of DHAA on phosphorylation of MEK1 and ERK1/2 (Figure 6K), BRAF V600E-MEK1 binding (Figure 6L) or cell proliferation rates assessed by IHC staining of Ki67 (Figures 6M and S6H) in tumors derived from A375 cells in mice. These data are consistent with previous results (Figures 5D–5E, S5C, 5I) showing that acetoacetate was insufficient to reverse the effect of DHAA on BRAF V600E-expressing cells.

DHAA reverses effect of dietary fat on BRAF V600E tumor growth

Consistent with our findings presented above, we found that treatment with a high-fat diet promoted, while DHAA alone inhibited, tumor growth rates, sizes and masses in nude mice with BRAF V600E-expressing A2058 or A375 cell xenografts, whereas co-treatment with DHAA effectively reversed the enhanced tumor growth potential of A2058 or A375 cells in xenograft mice fed with a high-fat diet (Figures 7A and S7A). A high-fat diet in the presence or absence of DHAA treatment did not affect body weight (Figure S7B). Although DHAA treatment had no effect on serum levels of acetoacetate, cholesterol, glucose or 3HB levels in mice fed with high-fat or normal foods (Figures 7B–7C and S7C–S7D, respectively), DHAA significantly attenuated the high-fat diet-dependent enhancement of phosphorylation of MEK1 and ERK1/2 (Figure 7D), BRAF V600E-MEK1 binding (Figure 7E), and cell proliferation rates assessed by IHC staining of Ki67 (Figures 7F and S7E) in tumors derived from A2058 and A375 cells. These results suggest that dietary fat likely promotes BRAF V600E tumor growth through regulation of serum levels of acetoacetate *in vivo*.

DISCUSSION

These findings reveal a pathologic link between a dietary component and specific oncogenic mutations that occur in human cancers, where the selective effect of dietary fat on BRAF V600E tumor growth is mediated through elevated ketogenesis and consequently increased circulating levels of acetoacetate. These studies provide insights into development of a concept that, by analogy to precision medicine, we term the “precision diet”, which is designed based on individual genetic background to lower cancer risk and provide cancer prevention. Thus, deciphering the molecular mechanisms by which certain dietary factors fuel cancer risk and disease development in patients with particular genetic alterations has highly impactful clinical significance. Furthermore, limiting dietary fat intake and monitoring circulating acetoacetate levels might be beneficial in patients with BRAF V600E melanoma or other related cancers and in individuals with BRAF V600E-positive premalignant lesions. In addition, it is plausible that lipid lowering agents may have a role in cancer prevention and/or supplemental treatment approaches to reduce cancer progression and/or improve clinical outcome in both the BRAF V600E-positive pre-malignancy and cancer settings. Obesity has been associated with an increased risk of malignant melanoma, which is approximately twice that in non-obese individuals, and worsens prognosis of malignant melanoma in diverse epidemiological and clinical studies (Amjadi et al., 2011; Antoniadis et al., 2011; Brandon et al., 2009; Chen et al., 2013; Dennis et al., 2008; Kirkpatrick et al., 1994; Oh et al., 2005; Pandey et al., 2012; Sergentanis et al., 2013; Shors et al., 2001). A recent study also links fat mass and obesity-associated (FTO), a gene associated with obesity and overeating, with an increased risk of malignant melanoma (Iles et al., 2013). Interestingly, Sergentanis et al reported that a 31% increased risk of malignant

melanoma was observed among overweight and obese men, whereas no significant changes were observed for obese women (Sergentanis et al., 2013). However, none of these studies was controlled for BRAF V600E mutational status of individuals. Higher-order associations between obesity and risk of BRAF V600E-positive malignant melanoma should be addressed and examined by future studies.

Interestingly, changes of circulating acetoacetate at sub-millimolar levels are sufficient to alter BRAF V600E tumor growth *in vivo*, whereas acetoacetate treatment in millimolar level is required to promote cell proliferation of cultured BRAF V600E tumor cells *in vitro*. Such response disparity might be due to that, in the *in vitro* cell proliferation assay, cells are cultured in complete media with various growth factors and abundant nutrients that provide an optimized culture condition for cells to achieve almost maximized cell proliferation potential, whereas cells in growing tumors likely are not provided with such optimized conditions. This might explain why the cultured cells are less sensitive to acetoacetate treatment in terms of enhanced cell proliferation. Moreover, tumor formation and growth in animals at the whole organism level are complex processes not just involving cell proliferation potential, so it is possible that other related processes including, for example, tumorigenesis and angiogenesis might be more sensitive to the change of circulating acetoacetate level.

Hymeglusin (Skaff et al., 2012; Tomoda et al., 2004) and 3-hydroxyglutaryl-CoA (Fu et al., 2010) have been reported as inhibitors of two key ketogenic enzymes, HMG-CoA synthase (HMGCS) and HMGCL, respectively. Future anti-ketogenic drugs such as small molecule inhibitors of HMGCS and HMGCL, as well as DHAA and its next generation derivatives may represent alternative clinical treatments for patients with BRAF V600E-positive cancer. Although DHAA as a synthetic compound has been safely used as a fungicide and bactericide (Stedman et al., 1954), inhibition of ketogenesis and/or acetoacetate function may affect organs including the heart and brain that use ketone bodies including acetoacetate and 3HB for energy during fasting (Cotter et al., 2013; Morris, 2005). In addition, targeting HMGCL may cause side effects similar to the symptoms observed in patients with HMGCL deficiency (HMGCLD), which is caused by mutations in the HMGCL gene and represents a rare autosomal recessive inborn disease seen in infant patients during the first year of their life. The disease is characterized by metabolism errors including disruption of ketogenesis and L-leucine catabolism with acute clinical symptoms such as vomiting, seizures, metabolic acidosis, hypoketotic hypoglycemia, and lethargy (Menao et al., 2009). These concerns warrant further detailed toxicity and pharmacokinetics studies to evaluate potential anti-ketogenic or anti-acetoacetate therapies in clinical BRAF V600E-positive cancer treatment.

Our study also raises additional questions. For example, most foods contain several different kinds of fat. It is crucial to determine which type(s) of dietary fat are essential for ketogenesis and in particular acetoacetate production, and may be considered harmful dietary fats that should be eliminated from the diet of individuals with BRAF V600E-positive cancer or pre-malignancy. In addition, these mouse studies were performed within a relatively short time of less than 5 weeks. Future studies are warranted to examine the potential long term effects of treatments with high fat diet, ketone bodies, lipid lowering

agents, or DHAA on tumor growth potential of BRAF V600E positive and negative tumor cells *in vivo*. Interestingly, high-fat diet induced an increase in serum concentrations of 3HB in C57BL/6 mice ((Kennedy et al., 2007) and Figure S7F), whereas high-fat diet did not significantly affect serum concentrations of 3HB in Balb/c nude mice (Figure S7F). These data suggested that different mouse strains respond differently to the high-fat diet in terms of serum 3HB levels, which is likely due to the relatively low basal levels of serum 3HB in C57BL/6 mice prior to high fat food treatment, and that the basal level of serum 3HB in Balb/c nude mice may already represent a maximum physiological level for mice (Figure S7F). Future studies are warranted to include consideration of species and strain difference.

EXPERIMENTAL PROCEDURES

Thermal melt shift assays

The thermal melt shift assay was performed as previously described (Hitosugi et al., 2012). In brief, thermal shift assay of compound (DHAA)-protein (BRAF WT or BRAF V600E) interaction was performed in 96-well PCR plates with various compound concentrations and 200 μg/ml protein in a buffer solution (20 mM Tris, 100 mM NaCl, pH 7.4). SYPRO orange was used as a dye to monitor the fluorescence change at 610 nm. DHAA was dissolved in double distilled water and added to the protein solution. The cellular thermal shift assay was performed as previously described (Martinez Molina et al., 2013). Briefly, 293T cells were transfected with FLAG-BRAF-WT or V600E mutant. After 24 h, cells were collected, resuspended in TBS and lysed with three cycles of freeze-thaw using dry ice/ethanol slurry. The soluble fraction was separated by centrifugation at 18,000g for 20 min. The cell lysates were then incubated with vehicle control, AA (400 μM) or DHAA (400 μM) for 15 min at room temperature. Subsequently, the lysates were aliquoted into 9 PCR tubes and heated at 46, 49, 52, 55, 58, 61, 64, 67 and 70°C for 3 min. The precipitated proteins were removed by centrifugation at 18,000g for 20 min and the soluble proteins were subjected to Western blot analysis.

^{14}C-acetoacetate and BRAF binding assay

Purified recombinant BRAF protein variants were pre-bound with FLAG-beads, followed by incubating with the indicated concentrations of ^{14}C-labeled acetoacetate (American Radiolabeled Chemicals) in 1xTBS (50 mM Tris, 150 mM NaCl, pH 7.5) buffer for 4 h at 4°C. The appropriate amount of DHAA as previously described was then added into the reaction mixture to incubate for another 4 h at 4°C. Alternatively, bead-bound BRAF protein variants were incubated first with the indicated concentrations of DHAA in 1xTBS buffer for 4 h at 4°C, then the appropriate amount of ^{14}C-labeled acetoacetate as previously described was added into the reaction mixture to incubate for another 4 h at 4°C. The beads were then washed and bead-bound BRAF proteins were eluted by incubating with 10 μg 3xFLAG peptides (Sigma-Aldrich) for 1 h. Radioactive signals of BRAF-bound ^{14}C-labeled acetoacetate were detected by liquid scintillation counting. Kd values were calculated using GraphPad Prism Software. For measurement of Ki of DHAA to BRAF in the presence of ^{14}C-acetoacetate. Bead-bound FLAG-BRAF variants were incubated with 300 μM ^{14}C-acetoacetate in TBS buffer for 4 h at 4°C, followed by further incubation with 0, 10, 20, 50, 100, 200, 500, 1000 μM DHAA for another 4 h at 4°C after unbound ^{14}C-acetoacetate was

washed off. The bead-bound BRAF proteins were eluted with 10 μg FLAG peptides and the radioactivity of retained ^{14}C-acetoacetate on BRAF variants was detected by liquid scintillation counting. Ki values were calculated using GraphPad Prism Software.

Animal models

The design and conduct of all experiments using mice was approved by the Institutional Animal Care and Use Committee of Emory University. For xenograft studies, nude mice (nu/nu, female 4–6-week-old, Harlan Laboratories) were subcutaneously injected with 1×10^6 melanoma cells on the flank. Tumor growth was recorded every two days from one week after inoculation by measurement of two perpendicular diameters using the formula $4\pi/3$ x (width/2)^2 x (length/2). Mice were sacrificed ~4 weeks after inoculation. The masses of tumors (g) derived from treatments were compared. Statistical analyses were performed by comparison in relation to the control group with a two-tailed paired Student's *t* test. Mice in the high-fat diet group started receiving paste high-fat diet (Bio serv F3666) or solid high-fat diet (Research Diets D12369B) one week before tumor cell inoculation and continued to receive the diet until the experimental endpoint. Mice in the control group received standard rodent diet (LabDiet 5015).

The amount of solid high-fat diet and standard diet consumed by mice was recorded by weighing the food mass. Body weights of mice were recorded weekly. AA (100mg/kg/day), 3HB (100mg/kg/day), DHAA (200mg/kg/day) and LiCl (42mg/kg/day) were injected into mice intraperitoneally daily beginning on the day of tumor inoculation. Lipid lowering agents (fenofibrate (200mg/kg/day), niacin (200mg/kg/day), or fluvastatin (40mg/kg/day)) were given to mice by oral gavage beginning on the day of tumor inoculation and AA (100mg/kg/day) was intraperitoneally injected beginning on the same day. For gut microbiome analysis, nude mice were injected with DHAA (200mg/kg/day) for 4 weeks before feces collection. Feces from each mouse in the same cage were collected and mixed as one sample. ~100mg feces from each cage were sent to GENEWIZ company for 16S rRNA sequencing and gut microbiome analysis.

Measurements of acetoacetate, 3HB, cholesterol, glucose and triglyceride

Acetoacetate levels in mouse serum and urine samples and tumor lysates were measured using the Acetoacetate Colorimetric Assay Kit (BioVision) following the manufacturer's instructions. In brief, serum, urine or tumor lysates were incubated with acetoacetate substrate at room temperature for 10 minutes. The alteration in absorbance (OD550) was measured in a kinetic mode. 3HB levels in mouse serum and urine samples were measured using the Ketone Body Assay Kit (Abnova) following the manufacturer's instructions. In brief, serum, urine or tumor lysates were incubated with cholesterol esterase, probe and enzyme mix provided in the kit for 60 minutes at 37 °C in dark. Alteration in absorbance at OD570 was measured. For cholesterol assay, total cholesterol levels in mouse serum samples were measured using the Total Cholesterol and Cholesteryl Ester Colorimetric/Fluorometric Assay Kit (Biovision) following the manufacturer's instructions. In brief, serum samples were incubated with cholesterol esterase, probe and enzyme mix provided in the kit for 60 minutes at 37 °C in dark. Alteration in absorbance at OD570 was measured. Glucose levels in mouse serum samples were measured using the Glucose Colorimetric/Fluorometric Assay

Kit (Biovision) following the manufacturer's instructions. In brief, serum samples were incubated with glucose probe and enzyme mix provided in the kit for 30 minutes at 37 °C in dark. Alteration in absorbance at OD570 was measured. Triglyceride levels in mouse serum samples were measured using the Triglyceride Quantification Colorimetric/Fluorometric Kit (Biovision) following the manufacturer's instructions. In brief, serum samples were pre-incubated with lipase at room temperature for 20 minutes in dark. Then triglyceride probe and enzyme mix provided in the kit were added and incubated for 60 minutes at room temperature in dark. Alteration in absorbance at OD570 was measured.

Supplementary Material

Refer to Web version on PubMed Central for supplementary material.

Acknowledgments

We thank Anthea Hammond for critical reading and editing of the manuscript. This work was supported in part by NIH grants CA140515, CA183594, CA174786 (J.C.), AR47901 (J.L.A.), Joel A. Katz Music Medicine Fund supported by the T.J. Martell Foundation/Winship Cancer Institute (J.C. and R.L.), the Jamie Rabinowitch Davis Foundation (J.L.A.), the Charles Harris Run For Leukemia, Inc. (H.J.K.), Melanoma Research Foundation and Winship Cancer Institute Melanoma & Skin cancer fund (B.P.P.). J.C. is a Winship 5K Scholar.

REFERENCES

Amjadi F, Javanmard SH, Zarkesh-Esfahani H, Khazaei M, Narimani M. Leptin promotes melanoma tumor growth in mice related to increasing circulating endothelial progenitor cells numbers and plasma NO production. J Exp Clin Cancer Res. 2011; 30:21. [PubMed: 21338489]

Antoniadis AG, Petridou ET, Antonopoulos CN, Dessypris N, Panagopoulou P, Chamberland JP, Adami HO, Gogas H, Mantzoros CS. Insulin resistance in relation to melanoma risk. Melanoma Res. 2011; 21:541–546. [PubMed: 21946019]

Arcaini L, Zibellini S, Boveri E, Riboni R, Rattotti S, Varettoni M, Guerrera ML, Lucioni M, Tenore A, Merli M, Rizzi S, Morello L, Cavalloni C, Da Via MC, Paulli M, Cazzola M. The BRAF V600E mutation in hairy cell leukemia and other mature B-cell neoplasms. Blood. 2012; 119:188–191. [PubMed: 22072557]

Avis HJ, Vissers MN, Stein EA, Wijburg FA, Trip MD, Kastelein JJ, Hutten BA. A systematic review and meta-analysis of statin therapy in children with familial hypercholesterolemia. Arterioscler Thromb Vasc Biol. 2007; 27:1803–1810. [PubMed: 17569881]

Balasse EO, Fery F. Ketone body production and disposal: effects of fasting, diabetes, and exercise. Diabetes Metab Rev. 1989; 5:247–270. [PubMed: 2656155]

Benlloch S, Paya A, Alenda C, Bessa X, Andreu M, Jover R, Castells A, Llor X, Aranda FI, Massuti B. Detection of BRAF V600E mutation in colorectal cancer: comparison of automatic sequencing and real-time chemistry methodology. J Mol Diagn. 2006; 8:540–543. [PubMed: 17065421]

Bollag G, Tsai J, Zhang J, Zhang C, Ibrahim P, Nolop K, Hirth P. Vemurafenib: the first drug approved for BRAF-mutant cancer. Nature reviews. Drug discovery. 2012; 11:873–886. [PubMed: 23060265]

Brandon EL, Gu JW, Cantwell L, He Z, Wallace G, Hall JE. Obesity promotes melanoma tumor growth: role of leptin. Cancer biology & therapy. 2009; 8:1871–1879. [PubMed: 19713740]

Brummer T, Martin P, Herzog S, Misawa Y, Daly RJ, Reth M. Functional analysis of the regulatory requirements of B-Raf and the B-Raf(V600E) oncoprotein. Oncogene. 2006; 25:6262–6276. [PubMed: 16702958]

Chapman MA, Lawrence MS, Keats JJ, Cibulskis K, Sougnez C, Schinzel AC, Harview CL, Brunet JP, Ahmann GJ, Adli M, Anderson KC, Ardlie KG, Auclair D, Baker A, Bergsagel PL, Bernstein BE, Drier Y, Fonseca R, Gabriel SB, Hofmeister CC, Jagannath S, Jakubowiak AJ, Krishnan A, Levy J, Liefeld T, Lonial S, Mahan S, Mfuko B, Monti S, Perkins LM, Onofrio R, Pugh TJ, Rajkumar SV, Ramos AH, Siegel DS, Sivachenko A, Stewart AK, Trudel S, Vij R, Voet D, Winckler W,

Zimmerman T, Carpten J, Trent J, Hahn WC, Garraway LA, Meyerson M, Lander ES, Getz G, Golub TR. Initial genome sequencing and analysis of multiple myeloma. Nature. 2011; 471:467–472. [PubMed: 21430775]

Chen J, Chi M, Chen C, Zhang XD. Obesity and melanoma: exploring molecular links. Journal of cellular biochemistry. 2013; 114:1955–1961. [PubMed: 23554059]

Cotter DG, Schugar RC, Crawford PA. Ketone body metabolism and cardiovascular disease. Am J Physiol Heart Circ Physiol. 2013; 304:H1060–H1076. [PubMed: 23396451]

Dennis LK, Lowe JB, Lynch CF, Alavanja MC. Cutaneous melanoma and obesity in the Agricultural Health Study. Ann Epidemiol. 2008; 18:214–221. [PubMed: 18280921]

Fu Z, Runquist JA, Montgomery C, Miziorko HM, Kim JJ. Functional insights into human HMG-CoA lyase from structures of Acyl-CoA-containing ternary complexes. J Biol Chem. 2010; 285:26341–26349. [PubMed: 20558737]

Gibney GT, Messina JL, Fedorenko IV, Sondak VK, Smalley KS. Paradoxical oncogenesis--the long-term effects of BRAF inhibition in melanoma. Nat Rev Clin Oncol. 2013; 10:390–399. [PubMed: 23712190]

Greenwald P, Clifford CK, Milner JA. Diet and cancer prevention. European journal of cancer. 2001; 37:948–965. [PubMed: 11334719]

Hay RWBMA. Kinetics of the Decarboxylation of Acetoacetic acid. Australian Journal of Chemistry. 1967; 20:1823–1828.

Hitosugi T, Zhou L, Elf S, Fan J, Kang HB, Seo JH, Shan C, Dai Q, Zhang L, Xie J, Gu TL, Jin P, Aleckovic M, Leroy G, Kang Y, Sudderth JA, Deberardinis RJ, Luan CH, Chen GZ, Muller S, Shin DM, Owonikoko TK, Lonial S, Arellano ML, Khoury HJ, Khuri FR, Lee BH, Ye K, Boggon TJ, Kang S, He C, Chen J. Phosphoglycerate mutase 1 coordinates glycolysis and biosynthesis to promote tumor growth. Cancer Cell. 2012; 22:585–600. [PubMed: 23153533]

Iles MM, Law MH, Stacey SN, Han J, Fang S, Pfeiffer R, Harland M, Macgregor S, Taylor JC, Aben KK, Akslen LA, Avril MF, Azizi E, Bakker B, Benediktsdottir KR, Bergman W, Scarra GB, Brown KM, Calista D, Chaudru V, Fargnoli MC, Cust AE, Demenais F, de Waal AC, Debniak T, Elder DE, Friedman E, Galan P, Ghiorzo P, Gillanders EM, Goldstein AM, Gruis NA, Hansson J, Helsing P, Hocevar M, Hoiom V, Hopper JL, Ingvar C, Janssen M, Jenkins MA, Kanetsky PA, Kiemeney LA, Lang J, Lathrop GM, Leachman S, Lee JE, Lubinski J, Mackie RM, Mann GJ, Martin NG, Mayordomo JI, Molven A, Mulder S, Nagore E, Novakovic S, Okamoto I, Olafsson JH, Olsson H, Pehamberger H, Peris K, Grasa MP, Planelles D, Puig S, Puig-Butille JA, Randerson-Moor J, Requena C, Rivoltini L, Rodolfo M, Santinami M, Sigurgeirsson B, Snowden H, Song F, Sulem P, Thorisdottir K, Tuominen R, Van Belle P, van der Stoep N, van Rossum MM, Wei Q, Wendt J, Zelenika D, Zhang M, Landi MT, Thorleifsson G, Bishop DT, Amos CI, Hayward NK, Stefansson K, Bishop JA, Barrett JH. A variant in FTO shows association with melanoma risk not due to BMI. Nature genetics. 2013; 45:428–432. 432e421. [PubMed: 23455637]

Jacobson TA, Chin MM, Fromell GJ, Jokubaitis LA, Amorosa LF. Fluvastatin with and without niacin for hypercholesterolemia. Am J Cardiol. 1994; 74:149–154. [PubMed: 8023779]

Johnson DB, Sosman JA. Update on the targeted therapy of melanoma. Current treatment options in oncology. 2013; 14:280–292. [PubMed: 23420410]

Kang HB, Fan J, Lin R, Elf S, Ji Q, Zhao L, Jin L, Seo JH, Shan C, Arbiser JL, Cohen C, Brat D, Miziorko HM, Kim E, Abdel-Wahab O, Merghoub T, Frohling S, Scholl C, Tamayo P, Barbie DA, Zhou L, Pollack BP, Fisher K, Kudchadkar RR, Lawson DH, Sica G, Rossi M, Lonial S, Khoury HJ, Khuri FR, Lee BH, Boggon TJ, He C, Kang S, Chen J. Metabolic Rewiring by Oncogenic BRAF V600E Links Ketogenesis Pathway to BRAF-MEK1 Signaling. Molecular cell. 2015; 59:345–358. [PubMed: 26145173]

Kennedy AR, Pissios P, Otu H, Roberson R, Xue B, Asakura K, Furukawa N, Marino FE, Liu FF, Kahn BB, Libermann TA, Maratos-Flier E. A high-fat, ketogenic diet induces a unique metabolic state in mice. Am J Physiol Endocrinol Metab. 2007; 292:E1724–E1739. [PubMed: 17299079]

Kim JW, Dang CV. Cancer's molecular sweet tooth and the Warburg effect. Cancer research. 2006; 66:8927–8930. [PubMed: 16982728]

Kirkpatrick CS, White E, Lee JA. Case-control study of malignant melanoma in Washington State. II. Diet, alcohol, and obesity. Am J Epidemiol. 1994; 139:869–880. [PubMed: 8166137]

Kroemer G, Pouyssegur J. Tumor cell metabolism: cancer's Achilles' heel. Cancer Cell. 2008; 13:472–482. [PubMed: 18538731]

Martinez Molina D, Jafari R, Ignatushchenko M, Seki T, Larsson EA, Dan C, Sreekumar L, Cao Y, Nordlund P. Monitoring drug target engagement in cells and tissues using the cellular thermal shift assay. Science. 2013; 341:84–87. [PubMed: 23828940]

McPherson PA, McEneny J. The biochemistry of ketogenesis and its role in weight management, neurological disease and oxidative stress. J Physiol Biochem. 2012; 68:141–151. [PubMed: 21983804]

Menao S, Lopez-Vinas E, Mir C, Puisac B, Gratacos E, Arnedo M, Carrasco P, Moreno S, Ramos M, Gil MC, Pie A, Ribes A, Perez-Cerda C, Ugarte M, Clayton PT, Korman SH, Serra D, Asins G, Ramos FJ, Gomez-Puertas P, Hegardt FG, Casals N, Pie J. Ten novel HMGCL mutations in 24 patients of different origin with 3-hydroxy-3-methyl-glutaric aciduria. Hum Mutat. 2009; 30:E520–E529. [PubMed: 19177531]

Miller AB. Diet and cancer. A review. Acta Oncol. 1990; 29:87–95. [PubMed: 2178651]

Morris AA. Cerebral ketone body metabolism. J Inherit Metab Dis. 2005; 28:109–121. [PubMed: 15877199]

Oh SW, Yoon YS, Shin SA. Effects of excess weight on cancer incidences depending on cancer sites and histologic findings among men: Korea National Health Insurance Corporation Study. Journal of clinical oncology : official journal of the American Society of Clinical Oncology. 2005; 23:4742–4754. [PubMed: 16034050]

Pandey V, Vijayakumar MV, Ajay AK, Malvi P, Bhat MK. Diet-induced obesity increases melanoma progression: involvement of Cav-1 and FASN. International journal of cancer. 2012; 130:497–508. [PubMed: 21387314]

Sebolt-Leopold JS, Herrera R. Targeting the mitogen-activated protein kinase cascade to treat cancer. Nature reviews. Cancer. 2004; 4:937–947. [PubMed: 15573115]

Sergentanis TN, Antoniadis AG, Gogas HJ, Antonopoulos CN, Adami HO, Ekbom A, Petridou ET. Obesity and risk of malignant melanoma: a meta-analysis of cohort and case-control studies. European journal of cancer. 2013; 49:642–657. [PubMed: 23200191]

Shors AR, Solomon C, McTiernan A, White E. Melanoma risk in relation to height, weight, and exercise (United States). Cancer Causes Control. 2001; 12:599–606. [PubMed: 11552707]

Skaff DA, Ramyar KX, McWhorter WJ, Barta ML, Geisbrecht BV, Miziorko HM. Biochemical and structural basis for inhibition of Enterococcus faecalis hydroxymethylglutaryl-CoA synthase, mvaS, by hymeglusin. Biochemistry. 2012; 51:4713–4722. [PubMed: 22510038]

Stedman RL, Engel SL, Bilse IM. In vitro antimicrobial activity of a dehydroacetic acid and p-chlor-m-xylenol combination. J Am Pharm Assoc Am Pharm Assoc (Baltim). 1954; 43:622–624.

Superko HR. A review of combined hyperlipidaemia and its treatment with fenofibrate. J Int Med Res. 1989; 17:99–112. [PubMed: 2656334]

Tennant DA, Duran RV, Gottlieb E. Targeting metabolic transformation for cancer therapy. Nature reviews. Cancer. 2010; 10:267–277.

Tomoda H, Ohbayashi N, Morikawa Y, Kumagai H, Omura S. Binding site for fungal beta-lactone hymeglusin on cytosolic 3-hydroxy-3-methylglutaryl coenzyme A synthase. Biochimica et biophysica acta. 2004; 1636:22–28. [PubMed: 14984735]

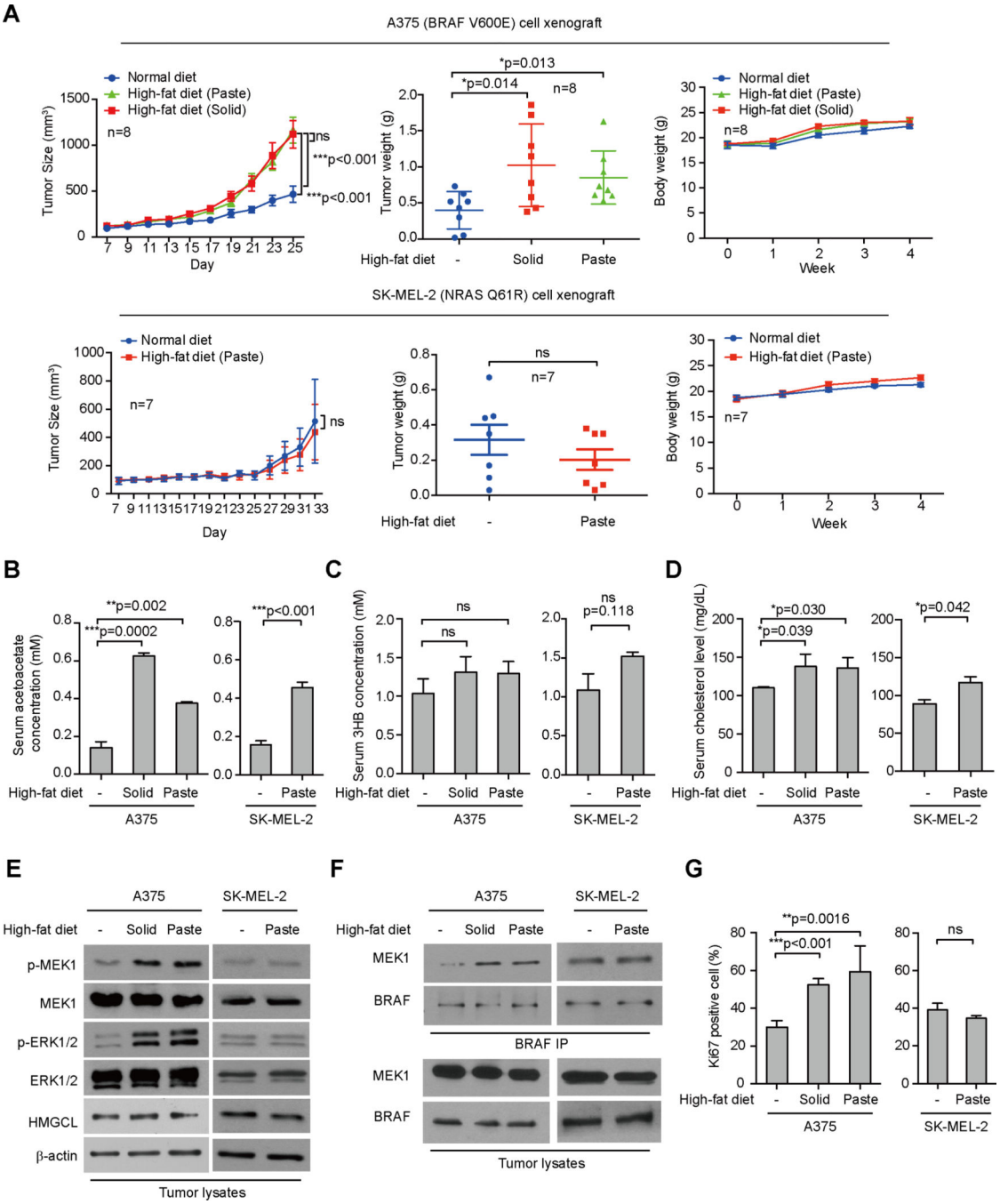

Figure 1. High-fat diet selectively promotes tumor growth potential of BRAF V600E-positive melanoma cells in xenograft nude mice

(A) Tumor growth (*left*), weight (*middle*) and body weight (*right*) of xenograft nude mice injected with human melanoma BRAF V600E-positive A375 (*upper* panels), or SK-MEL-2 cells (NRAS Q61K; *lower* panels) that were fed with normal diet, or different high-fat diets. Data are mean ± SEM for tumor growth and mean ± s.d. for tumor weight; *p* values were obtained by a two-way ANOVA test for tumor growth rates and a two-tailed Student's *t* test for tumor masses.

(B–D) Acetoacetate (AA; B), β-hydroxybutyrate (3HB; C), and cholesterol (D) levels in serum harvested from A375 and SK-MEL-2 xenograft mice fed with normal or different high-fat diets. Data are mean ± s.d.; n=3; *p* values were obtained by a two-tailed Student's *t* test.

(E–F) Western blot results show MEK1 and ERK1/2 phosphorylation (E) and BRAF-MEK1 binding (F) in tumor tissue samples obtained from xenograft mice.

(G) Summarized results of immunohistochemical (IHC) staining assay detecting Ki67-positive cells in tumor tissue samples from A375 and SK-MEL-2 xenograft mice. Data are mean ± s.d.; *p* values were obtained by a two-tailed Student's *t* test.

Also see Figure S1.

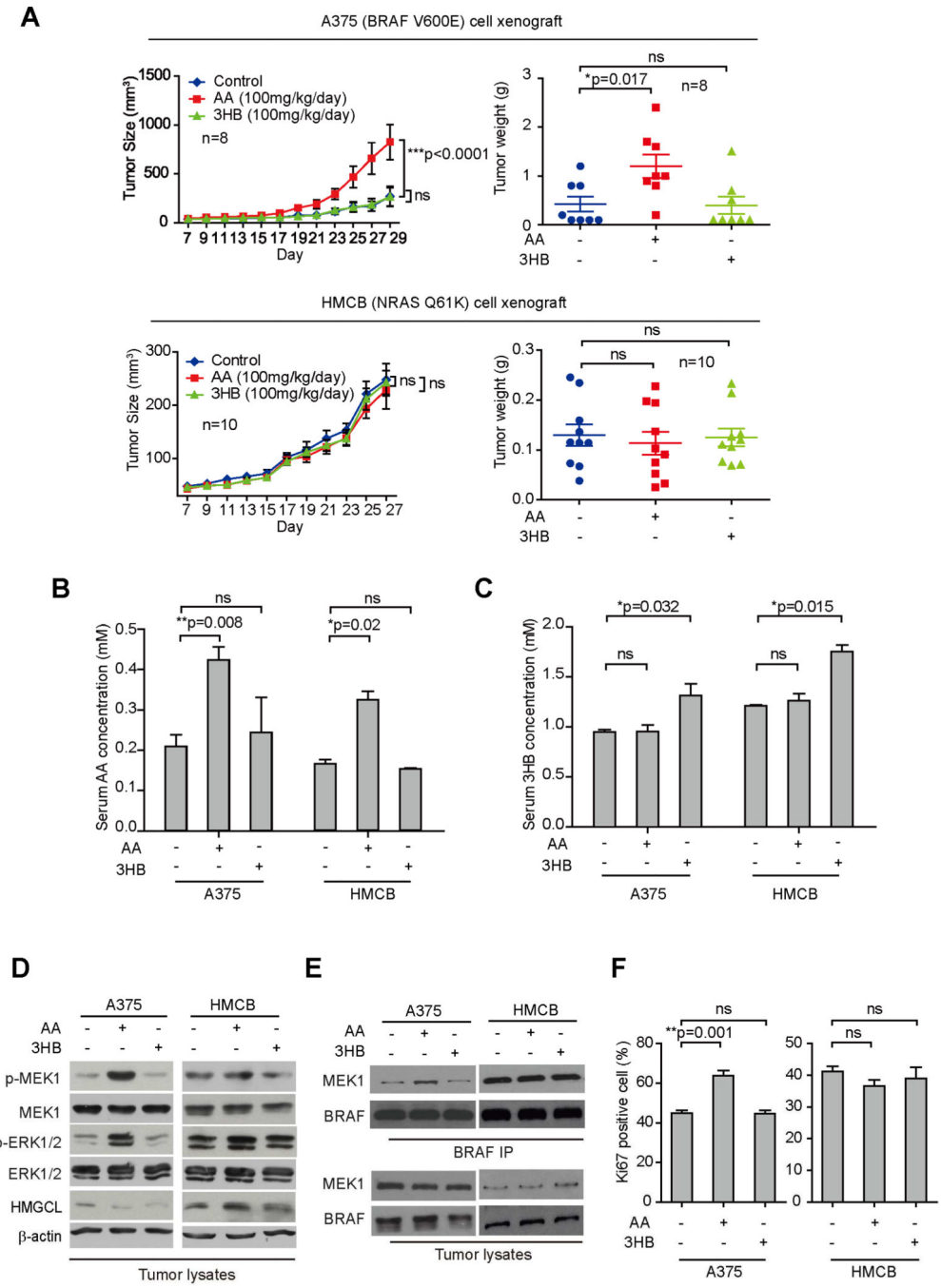

Figure 2. Intraperitoneally injected acetoacetate selectively promotes BRAF V600E-positive melanoma tumor growth

(A) Tumor growth (*left*) and weight (*right*) of xenograft nude mice injected with human melanoma BRAF V600E-positive A375 (*upper* panels) or HMCB (NRAS Q61K; *lower* panels) cells that were intraperitoneally injected with AA or 3HB. Data are mean ± SEM for tumor growth and mean ± s.d. for tumor weight; *p* values were obtained by a two-way ANOVA test for tumor growth rates and a two-tailed Student's *t* test for tumor masses.

(B–C) AA (B) and 3HB (C) levels in serum harvested from A375 and HMCB xenograft mice treated with AA or 3HB. Data are mean ± s.d.; n=3; *p* values were obtained by a two-tailed Student's *t* test.

(D–E) Western blot results show MEK1 and ERK1/2 phosphorylation (D) and BRAF-MEK1 binding (E) in tumor tissue samples obtained from xenograft mice.

(F) Summarized results of IHC staining assay detecting Ki67-positive cells in tumor tissue samples from xenograft mice. Data are mean ± s.d.; *p* values were obtained by a two-tailed Student's *t* test.

Also see Figure S2 and S3.

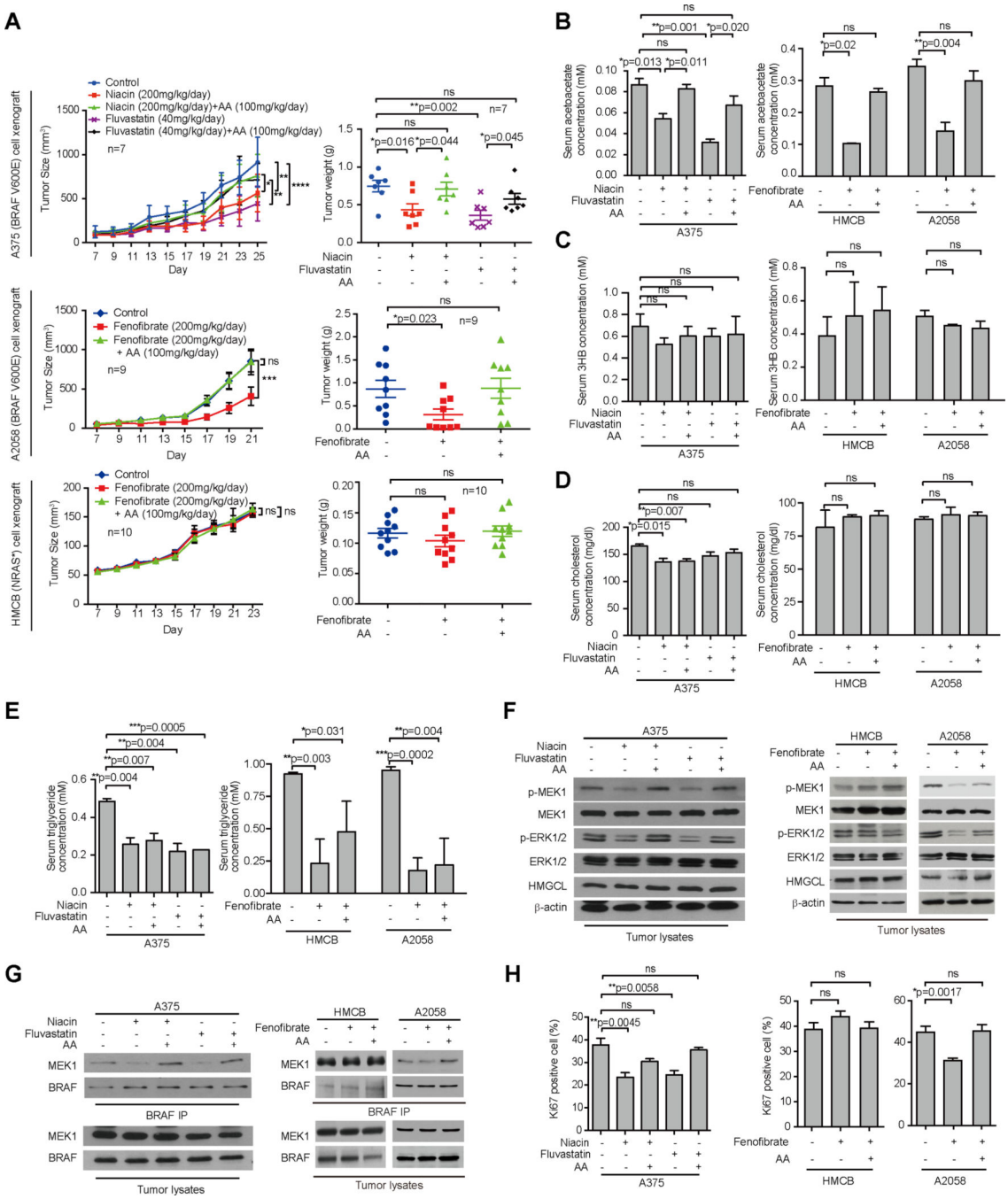

Figure 3. Lipid lowering agents decrease serum acetoacetate levels in xenograft mice and reduce VRAF V600E tumor growth

(A) Tumor growth (*left*) and weight (*right*) of xenograft nude mice injected with human melanoma BRAF V600E-positive A375 cells (*upper* panels) that were orally treated with two different lipid lowering agents Niacin or Fluvastatin alone or in combination with intraperitoneal injection with acetoacetate (AA); Tumor growth (*left*) and weight (*right*) of xenograft nude mice injected with human melanoma BRAF V600E-positive A2058 (*middle*) cells or HMCB (NRAS Q61K; *lower* panels) cells that were orally treated with lipid lowering agent Fenofibrate alone or in combination with intraperitoneal injection with AA.

Data are mean ± SEM for tumor growth and mean ± s.d. for tumor weight; *p* values were obtained by a two-way ANOVA test for tumor growth rates and a two-tailed Student's *t* test for tumor masses.

(B–E) AA(B), 3HB (C), cholesterol (D), and triglyceride (E) levels in serum harvested from A375, A2058 and HMCB xenograft mice tissue. Data are mean ± s.d.; n=3; *p* values were obtained by a two-tailed Student's *t* test.

(F–G) Western blot results show MEK1 and ERK1/2 phosphorylation (F) and BRAF-MEK1 binding (G) in tumor tissue samples obtained from xenograft mice tissue.

(H) Summarized results of IHC staining assay detecting Ki67-positive cells in tumor tissue samples from xenograft mice. Data are mean ± s.d.; n=3; *p* values were obtained by a two-tailed Student's *t* test.

Also see Figures S4.

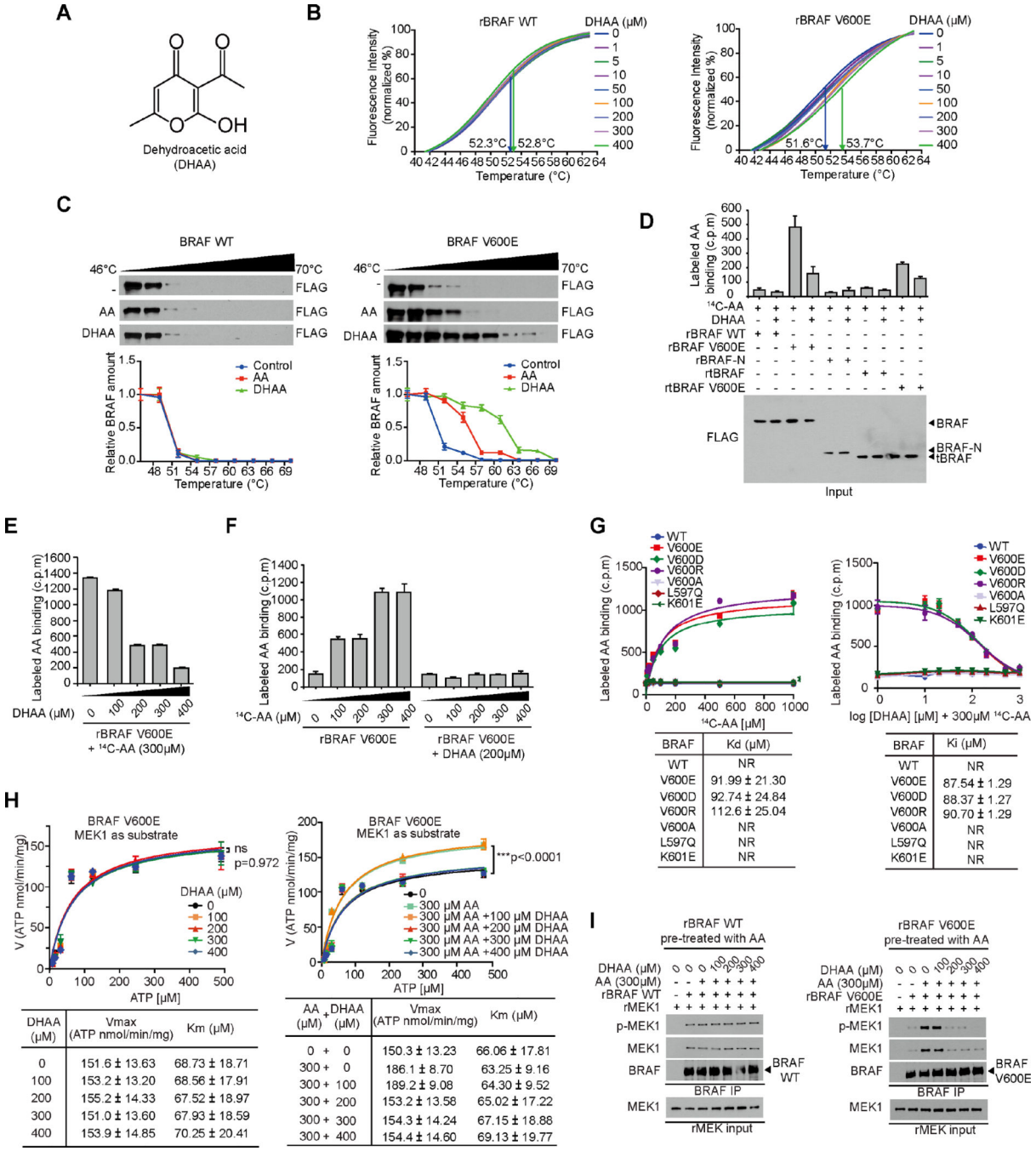

Figure 4. Dehydroacetic acid competes with acetoacetate for BRAF V600E binding and antagonizes acetoacetate-enhanced V600E-MEK1 association

(A) Chemical structure formula of dehydroacetic acid (DHAA).

(B) Thermal melt shift assay was performed to examine the protein (BRAF WT or BRAF V600E; *left* and *right* panel, respectively) and ligand (DHAA) interaction. Arrows in each panel indicate melting temperatures at 0 μM (*left*) and 400 μM (*right*).

(C) Intracellular thermal melt shift assay was performed to examine the protein (BRAF WT or BRAF V600E; *left* and *right* panel, respectively) and ligand (AA or DHAA) interaction.

(D) Radiometric metabolite-protein interaction analysis using ^{14}C-labeled acetoacetate incubated with purified BRAF variants, followed by treatment with DHAA. Data are mean ± s.d.; n=3 each; *p* values were obtained by a two-tailed Student's *t* test.

(E–F) Radiometric metabolite-protein interaction analysis using purified recombinant BRAF V600E (rBRAF V600E) pre-treated with ^{14}C-labeled acetoacetate incubated with increasing concentrations of DHAA (E), or rBRAF V600E pre-treated with DHAA incubated with increasing concentrations of ^{14}C-labeled acetoacetate (F). Data are mean ± s.d.; n=3 each; *p* values were obtained by a two-tailed Student's *t* test.

(G) Kd values (*left*) were determined by ^{14}C-labeled acetoacetate binding assay. BRAF wild type and mutant proteins were incubated with increasing concentrations of ^{14}C-labeled acetoacetate. Effect of increasing concentrations of DHAA on ^{14}C-labeled acetoacetate binding to BRAF mutant proteins (*right* panels).

(H) Vmax and Km of BRAF V600E were measured using purified BRAF V600E protein incubated with increasing concentrations of ATP in the presence and absence of increasing concentration of AA (*left* panel) or increasing concentration of DHAA with 300 μM AA (*right* panel), using excessive amount of purified MEK1 as substrates. Data are mean ± s.d.; n = 3 each; *p* values were obtained by a two-tailed Student's *t* test.

(I) Effect of increasing concentrations of DHAA on AA-enhanced rBRAF WT or rBRAF V600E binding to purified recombinant MEK1 (rMEK1).

Also see Figure S5.

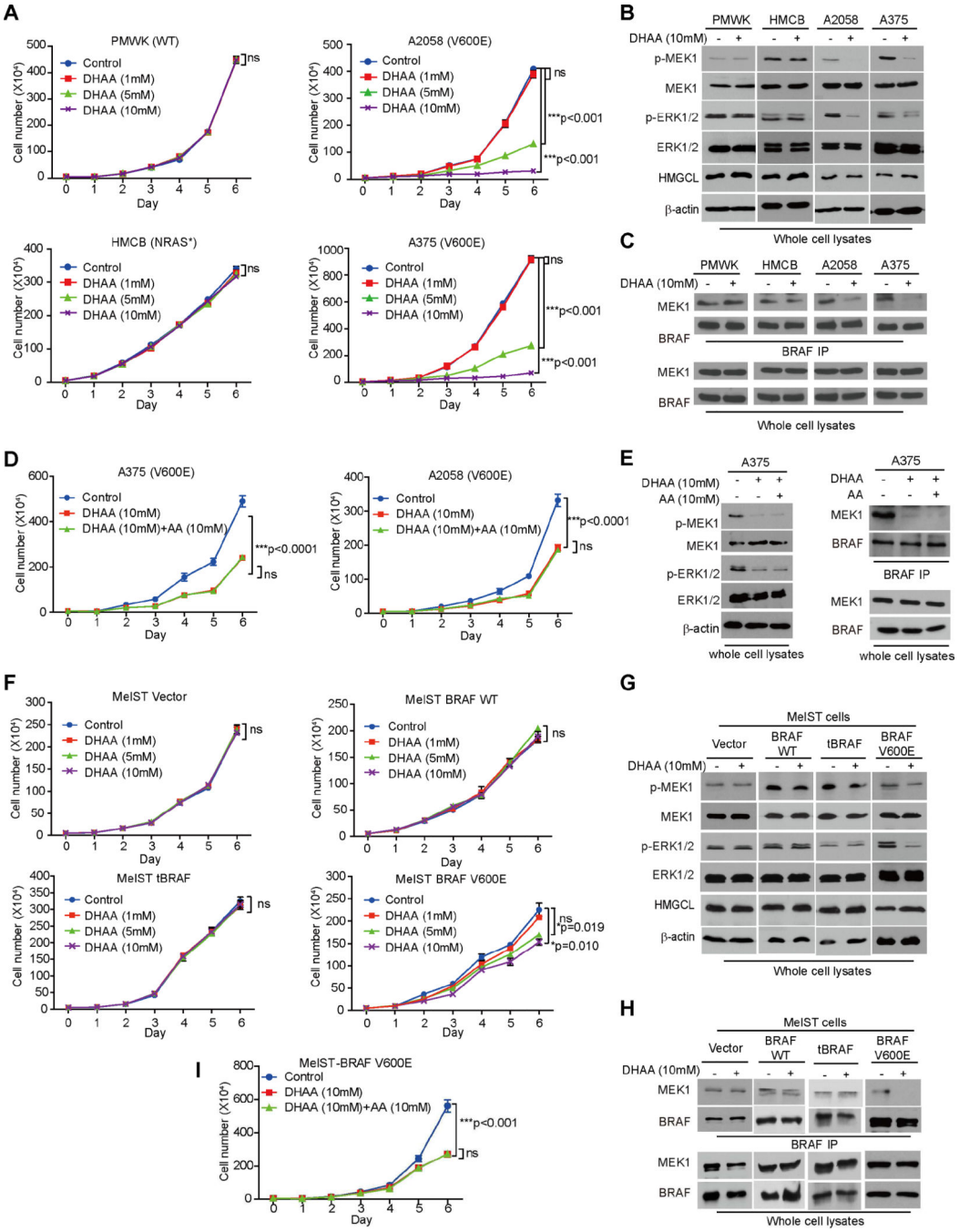

Figure 5. DHAA selectively inhibits BRAF V600E-positive melanoma cell proliferation

(A–C) Effect of DHAA treatment on cell proliferation rates (A), MEK1 and ERK1/2 phosphorylation (B) and BRAF-MEK1 binding (C) of melanoma PMWK, HMCB, A2058 and A375 cells. Data are mean ± s.d.; *p* values were obtained by a two-tailed Student's *t* test. (D–F) Effect of DHAA with or without AA treatment on cell proliferation rates (D), MEK1 and ERK1/2 phosphorylation (E), and BRAF-MEK1 binding (F) of melanoma BRAF-V600E positive A2058 and A375 cells. Data are mean ± s.d.; *p* values were obtained by a two-tailed Student's *t* test.

(G–I) Effect of DHAA treatment on cell proliferation rates (G), MEK1 and ERK1/2 phosphorylation (H) and BRAF-MEK1 binding (I) of Mel-ST cells stably expressing BRAF WT, BRAF V600E or a truncated, constitutively active form of BRAF (tBRAF). Data are mean ± s.d.; *p* values were obtained by a two-tailed Student's *t* test.

(I) Effect of DHAA with or without AA rescue treatment on cell proliferation rates Mel-ST cells stably expressing BRAF V600E. Data are mean ± s.d.; *p* values were obtained by a two-tailed Student's *t* test.

Also see Figures S5.

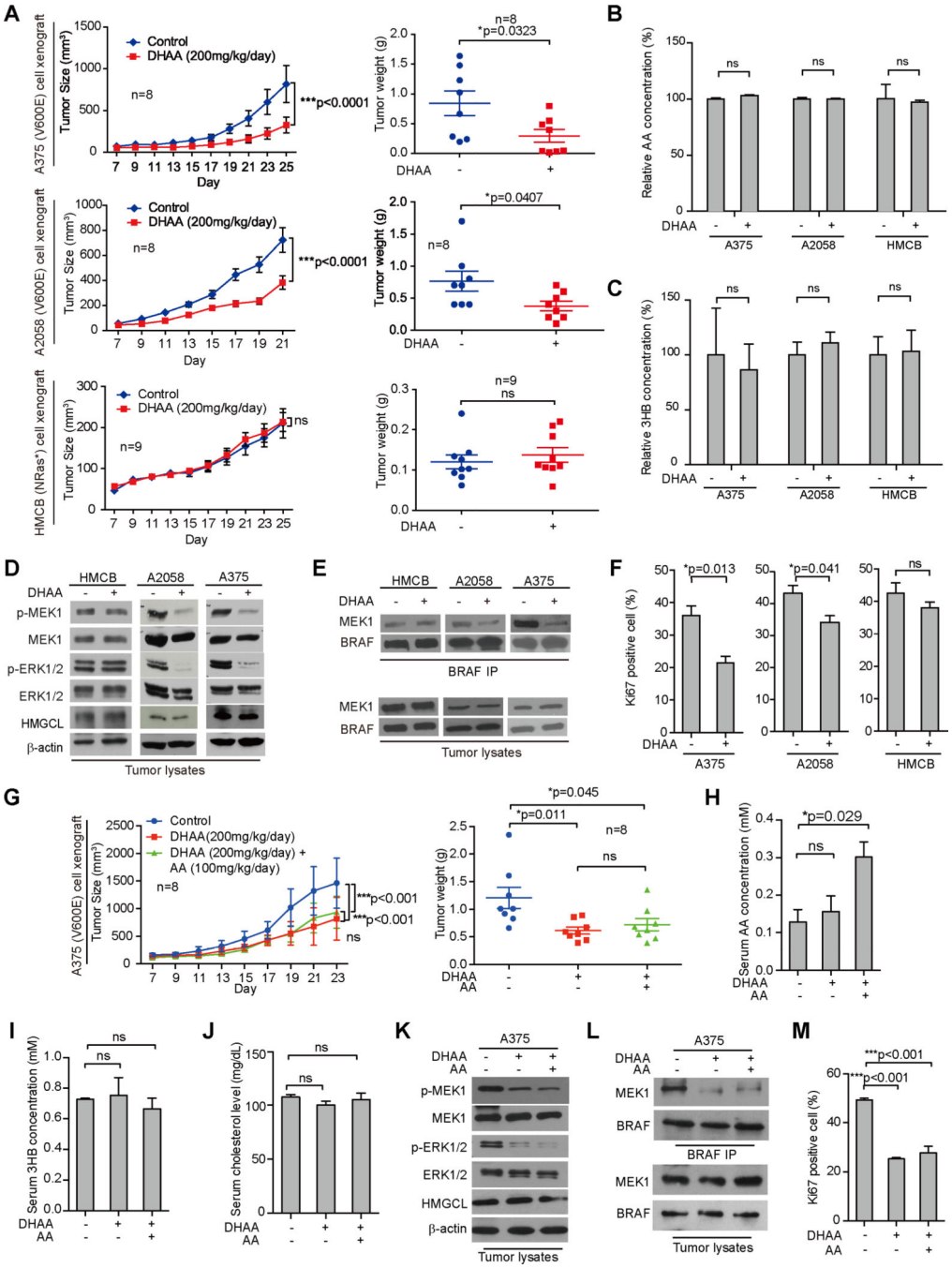

Figure 6. DHAA attenuates BRAF V600E tumor growth in xenograft nude mice

(A) Tumor growth (*left*) and weight (*right*) of xenograft nude mice injected with human melanoma BRAF V600E-positive A375 (*upper* panels) or A2058 (*middle* panels) and HMCB (NRAS Q61K; *lower* panels) cells were intraperitoneally injected with DHAA. Data are mean ± SEM for tumor growth and mean ± s.d. for tumor weight; p values were obtained by a two-way anova test and two-tailed Student's *t* test.

(B–C) AA (B) and 3HB (C) levels in tumor samples obtained from xenograft mice. Data are mean ± s.d.; n=3; p values were obtained by a two-tailed Student's *t* test.

(D–E) Western blot results assessing MEK1 and ERK1/2 phosphorylation (D) and BRAF-MEK1 binding (E) in tumor tissue samples obtained from xenograft mice.

(F) Summarized results of IHC staining assay detecting Ki67-positive cells in tumor tissue samples from xenograft mice. Data are mean ± s.d.; p values were obtained by a two-tailed Student's *t* test.

(G) Tumor growth (*left*) and weight (*right*) of xenograft nude mice injected with A375 were intraperitoneally injected with DHAA in the absence or presence of AA. Data are mean ± SEM for tumor growth and mean ± s.d. for tumor weight; *p* values were obtained by a two-way anova test and two-tailed Student's *t* test.

(H–J) AA (H), 3HB (I) and cholesterol (J) levels in tumor samples obtained from xenograft mice shown in (G). Data are mean ± s.d.; n=3; p values were obtained by a two-tailed Student's t test. (K–L) Western blot results assessing MEK1 and ERK1/2 phosphorylation (K) and BRAF-MEK1 binding (L) in tumor tissue samples obtained from xenograft mice shown in (G).

(H) Summarized results of IHC staining assay detecting Ki67-positive cells in tumor tissue samples from xenograft mice shown in (G). Data are mean ± s.d.; p values were obtained by a two-tailed Student's *t* test.

Also see Figure S6

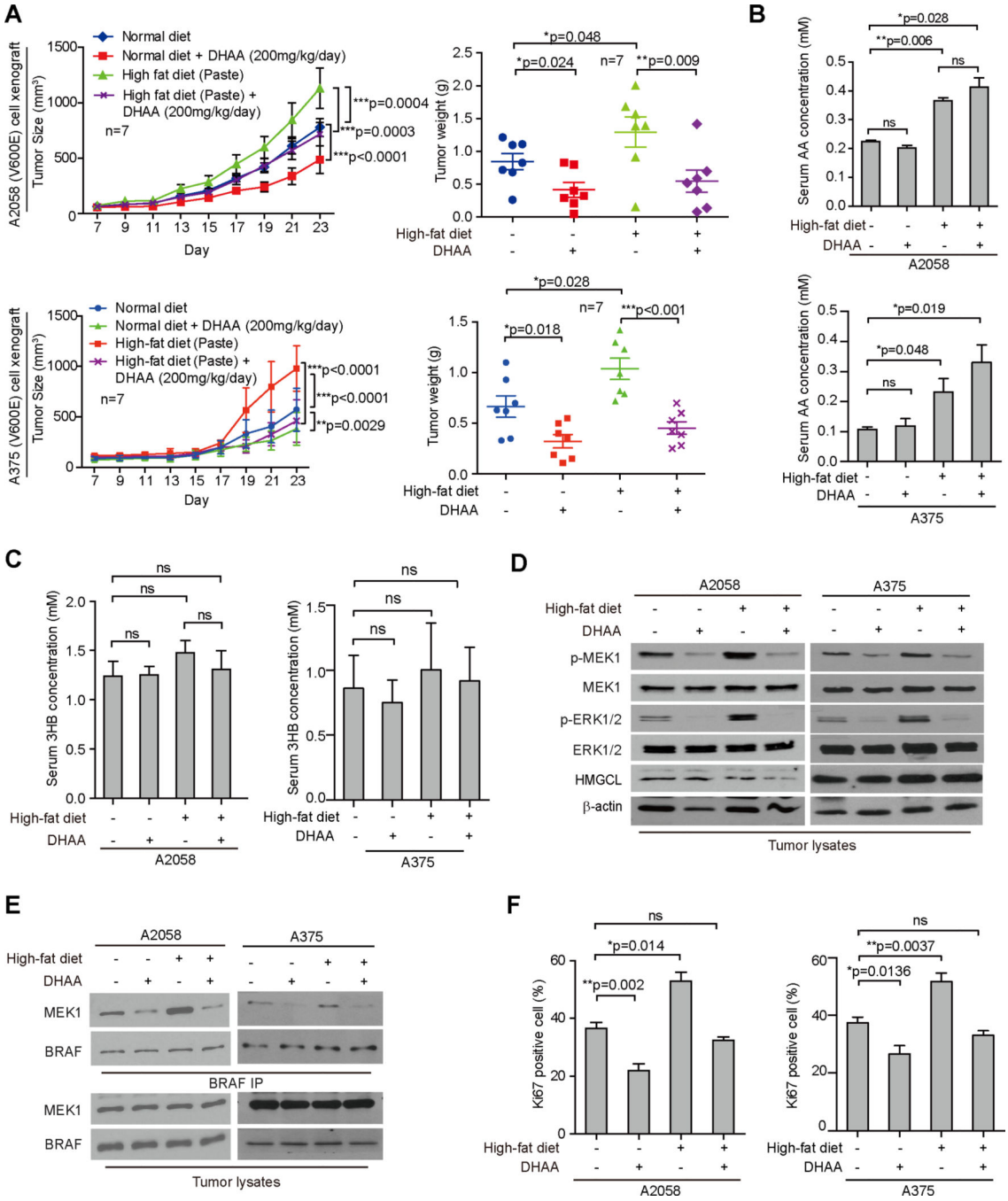

Figure 7. DHAA treatment reverses high-fat enhanced BRAF V600E tumor growth in xenograft nude mice

(A) Tumor growth (*left*) and weight (*right*) of xenograft nude mice injected with BRAF V600E-positive human melanoma A375 (*upper* panels) an A2058 (*bottom* panels) cells that were fed with normal or high-fat diets followed by intraperitoneal injection with DHAA. Data are mean ± SEM for tumor growth and mean ± s.d. for tumor weight; *p* values were obtained by a two-way ANOVA test.

(B–C) AA (B) and 3HB (C) levels in serum harvested from xenograft mice. Data are mean ± s.d.; n=3; *p* values were obtained by a two-way ANOVA test for tumor growth rates and a two-tailed Student's *t* test for tumor masses.

(D–E) Western blot results assessing MEK1 and ERK1/2 phosphorylation (D) and BRAF-MEK1 binding (E) in tumor tissue samples obtained from xenograft mice.

(F) Summarized results of IHC staining assay detecting Ki67-positive cells in tumor tissue samples from xenograft mice. Data are mean ± s.d.; *p* values were obtained by a two-tailed Student's *t* test.

Also see Figure S7.